Journal of Sound and Vibration (1998) **216**(5), 771–790
Article No. sv981720

EFFICIENCY OF A NOISE BARRIER ON THE GROUND WITH AN ACOUSTICALLY SOFT CYLINDRICAL EDGE

T. Okubo and K. Fujiwara

Deparment of Acoustic Design, *Kyushu Institute of Design*, 4-9-1 *Shiobaru*, *Minami-ku*, *Fukuoka* 815-8540, *Japan*

(*Received* 5 *May* 1997, *and in final form* 7 *April* 1998)

It is well-known that an absorptive obstacle installed on the edge of a noise barrier improves sound shielding efficiency without increasing the height of the barrier. This paper examines the sound shielding efficiency of a noise barrier with an acoustically "soft" cylindrical edge. "Soft" indicates that the sound pressure at the surface is zero; however, it is difficult to produce a soft surface using traditional materials. The authors previously reported that the "Waterwheel cylinder," which consists of acoustic tubes arranged radially, approximates a soft surface cylinder. In the present study, a noise barrier with a Waterwheel cylinder installed on the edge of the barrier is investigated. Results of numerical simulations indicated that the Waterwheel cylinder improves the sound shielding efficiency of a noise barrier. The improvement is strongly frequency dependent; it exceeds 10 dB in a certain frequency range of an octave, but the Waterwheel decreases the noise shielding efficiency in another frequency range. The frequency characteristics of the Waterwheel's effect are related to its cross-sectional shape. The Waterwheel improves the efficiency much better in the effective frequency range of an octave as compared with an absorbing cylinder. All numerical calculations were carried out assuming an unrealistic two-dimensional sound field, but results of scale model experiments indicate that the calculations predict very accurately the efficiency of noise barriers in a three-dimensional sound field.

1. INTRODUCTION

Several methods to improve the efficiency of a noise barrier without increasing the barrier height have been developed. Some of these methods are based on the idea of reducing the velocity potential around the edge of the barrier. It is well-known that the edge potential can be regarded as an imaginary line source for a diffracted field in the back of the barrier. Thus, suppression of the edge potential reduces the imaginary source, and consequently the diffracted field behind the barrier also decreases. Based on this concept, an absorptive obstacle installed on the barrier's edge has been proposed. According to one report, the installed absorber reduces the edge potential and improves the sound shielding efficiency of the noise barrier [1].

0022–460X/98/400791 + 20 $30.00/0

If one considers the edge potential as an imaginary source, additional suppression of the potential should further improve the sound shielding efficiency. Therefore, an obstacle with an "acoustic soft surface" [2] on the barrier's edge is expected to be effective. The characteristic impedance of a "soft surface" is sufficiently less than that of air, and consequently the surface sound pressure is much less than that on the absorptive surface. It has been theorized that a barrier with a soft cylindrical edge [3] and a barrier that is soft only around the edge [4] are efficient. These barriers are not widely used despite their significant effect because it is very difficult to obtain materials with an impedance significantly less than that of air. The authors have previously shown that the "Waterwheel cylinder" approximates a soft surface cylinder and that the sound shielding efficiency of a half plane improves with the Waterwheel installed on the edge [5]. This paper discusses the efficiency of a noise barrier sitting on the ground, with and without the Waterwheel cylinder.

2. DEVELOPMENT OF AN ACOUSTICALLY SOFT CYLINDER

As mentioned above, it is rather difficult to produce a soft surface. A soft surface can be produced, however, when the reflected wave has the same amplitude as that of the incident wave and the phase difference between them is equal to π. To produce a soft surface, Fujiwara proposed that one-quarter wavelength acoustic tubes be arranged in a plane [2]. Based on a similar notion, an obstacle was constructed whose cross-sectional shape is shown in Figure 1, to produce a soft surface cylinder [5]. This obstacle is referred to as a "Waterwheel cylinder" because of the shape of its cross-section, and use the concept of "the surface of the Waterwheel cylinder," which consists of open ends of tubes arranged radially.

Due to interference between the incident and reflected (travelling within a tube) waves, the sound pressure and the impedance on the surface of the Waterwheel depend on the wavelength of the incident wave. For example, if the tube depth corresponds to half of the wavelength, the Waterwheel's surface is almost acoustically hard because the phase difference is zero. That is, the Waterwheel cannot achieve a soft surface at all frequencies.

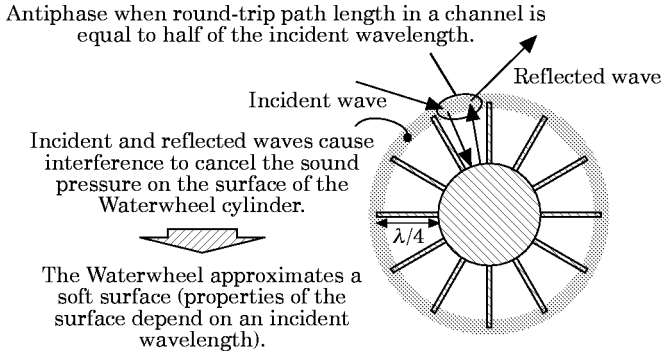

Figure 1. Development of a soft surface cylinder with the Waterwheel.

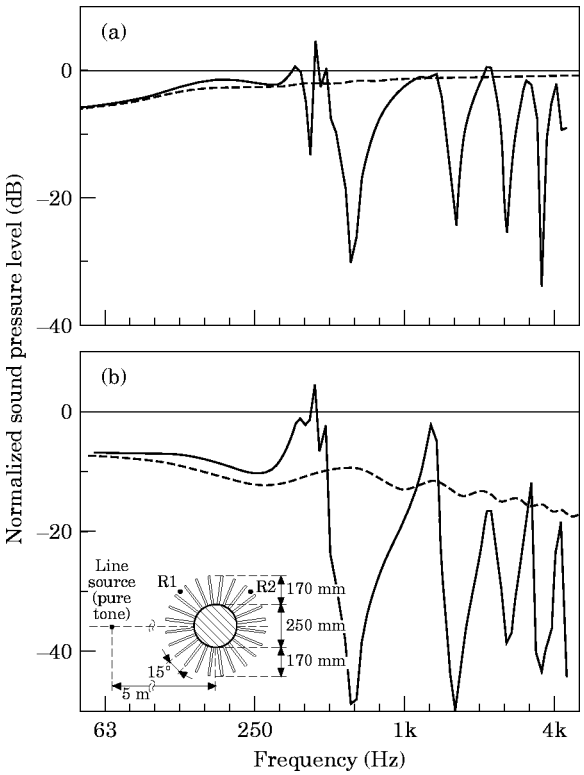

Figure 2. Frequency characteristics of the surface sound pressure on the isolated Waterwheel floating in a free field [5]: (a) at receiver R1, (b) at receiver R2. ——, the Waterwheel cylinder; - - - -, a rigid cylinder of the same diameter.

In the authors' previous report, numerical and experimental analyses of the sound field around the Waterwheel [5] were performed. Figure 2 shows typical examples of the frequency characteristics of the sound pressure level on the Waterwheel surface. It was found that the Waterwheel achieves a soft surface at a much higher frequency than expected. That is, the surface sound pressure of the Waterwheel whose channel depth is 170 mm vanishes at the frequencies $600 + 1000n$ Hz ($n = 0, 1, 2, \ldots$) approximately, while the depth corresponds to a quarter of the wavelength at 500 Hz. Because of interference, the acoustic properties of the Waterwheel's surface are unavoidably frequency dependent. Although it is obvious that the "acoustically soft" situation is obtained at the mouth of channels at a certain frequency, one cannot easily estimate the frequency that cancels the surface sound pressure because the channel is not rectangular, i.e., the mouth is larger than the bottom. Furthermore, it was found that the sound shielding efficiency of a half plane with the Waterwheel is also strongly frequency dependent. As a consequence, it is expected that the efficiency of the noise barrier on the ground is frequency dependent, corresponding to the surface sound pressure of the Waterwheel.

3. NUMERICAL ANALYSIS

In this section, the boundary integral equation and the boundary element method (BEM) briefly are described. A two-dimensional field is assumed throughout this paper, except in section 7 which describes the results of three-dimensional experiments, although the two-dimensional field is obviously not of practical interest. This is because the three-dimensional simulations require much more computational resources and calculation time. Figure 3 shows the cross-section of the situation for which the sound field was calculated. A two-dimensional field is assumed and thus the geometrical and acoustical variables are constant in the z direction. A noise barrier of infinite length lies on a rigid plane, i.e., on a reflective ground. The barrier and a monofrequency line source of sound are parallel to the z-axis. In section 7, it is shown that the two-dimensional analyses can be applied to a practical situation; that is, the three-dimensional situation where a point source and a receiver are in the vertical plane which is perpendicular to the axis of the noise barrier.

Let $\mathbf{r}_0$ denote the source position, $\mathbf{r}$ denote the receiver position, and $\beta(\mathbf{r}_s)$ denote the normalized surface admittance at point $\mathbf{r}_s$ on the barrier surface S. The sound pressure at the receiver, $p(\mathbf{r})$, satisfies the following boundary integral equation [6]:

$$\epsilon(\mathbf{r})p(\mathbf{r}, \mathbf{r}_0) = G(\mathbf{r}_0, \mathbf{r}) - \int_S \left(\frac{\partial G(\mathbf{r}_s, \mathbf{r})}{\partial n(\mathbf{r}_s)} + jk\beta(\mathbf{r}_s)G(\mathbf{r}_s, \mathbf{r}) \right) p(\mathbf{r}_s, \mathbf{r}_0)\, \mathrm{d}s(\mathbf{r}_s), \qquad (1)$$

where $\mathrm{d}s(\mathbf{r}_s)$ denotes the arc length of the barrier surface S at point $\mathbf{r}_s$, $\partial/\partial n(\mathbf{r}_s)$ denotes the normal derivative at $\mathbf{r}_s$, k denotes the wave number, and the time dependence factor $\exp(\mathrm{j}\omega t)$ is understood. $\epsilon(\mathbf{r}) = 1$ when $\mathbf{r}$ is in the propagating medium and not on S; $\epsilon(\mathbf{r}) = 1/2$ when $\mathbf{r}$ is on S. G is the sound pressure at $\mathbf{r}$ in the absence of the barrier:

$$G(\mathbf{r}, \mathbf{r}_0) = (1/4j)\{H_0^{(2)}(k|\mathbf{r}_0 - \mathbf{r}|) + H_0^{(2)}(k|\mathbf{r}_0' - \mathbf{r}|)\}, \qquad (2)$$

where $\mathbf{r}_0'$ denotes the position of the imaginary line source in the rigid ground, and $H_0^{(2)}$ is the Hankel function of the second kind of order zero.

In order to solve equation (1) numerically, the BEM was used. The barrier surface S was divided into straight elements $S_1, S_2, \ldots, S_N$, and $\mathbf{r}_n$ denotes the midpoint of S_n for $n = 1, 2, \ldots, N$. By the approximation that $p(\mathbf{r}, \mathbf{r}_0)$ is

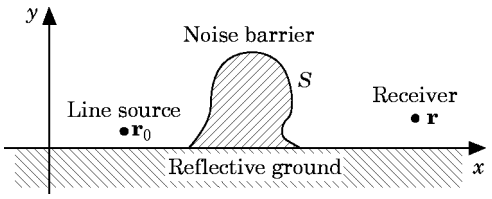

Figure 3. Cross-section of the two-dimensional sound field to be investigated by the boundary element method.

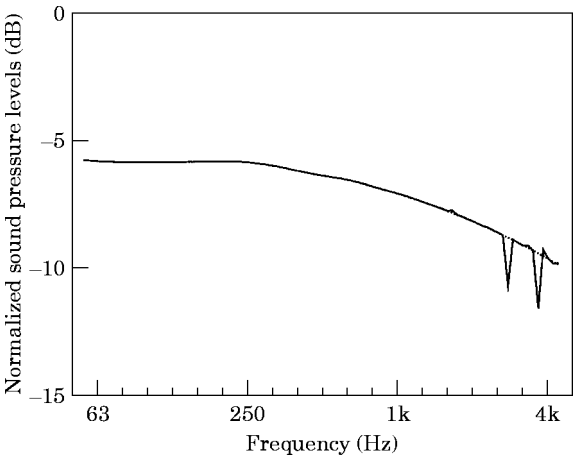

Figure 4. Comparison between BEM and an exact solution: SPL behind a hard circular cylinder. ——, BEM; . . . . , the exact solution.

constant and equal to $p(\mathbf{r}_n, \mathbf{r}_0)$ for $\mathbf{r}$ on S_n, equation (1) is written in the discrete form:

$$\epsilon(\mathbf{r})p(\mathbf{r}, \mathbf{r}_0) = G(\mathbf{r}_0, \mathbf{r}) - \sum_{n=1}^{N} p(\mathbf{r}_n, \mathbf{r}_0) \int_{S_n} \left(\frac{\partial G(\mathbf{r}_s, \mathbf{r})}{\partial n(\mathbf{r}_s)} + \mathrm{j}k\beta(\mathbf{r}_s)G(\mathbf{r}_s, \mathbf{r}) \right) \mathrm{d}s(\mathbf{r}_s). \quad (3)$$

Then by setting $\mathbf{r} = \mathbf{r}_m$ for $m = 1, 2, \ldots, N$ in equation (3), a set of N linear equations is obtained in the unknowns $p(\mathbf{r}_1, \mathbf{r}_0)$, $p(\mathbf{r}_2, \mathbf{r}_0)$, . . . , $p(\mathbf{r}_N, \mathbf{r}_0)$. When the equations are solved for $p(\mathbf{r}, \mathbf{r}_0)$, the sound pressure at any point $\mathbf{r}$, can be calculated by substituting the pressure at the midpoint of each element into equation (3). To solve the integral equation with sufficient accuracy, a maximum element length is smaller than $\lambda/8$ [7] in all of the calculations carried out in this paper.

To confirm the accuracy of the boundary element method, numerical simulations for some cases were carried out using the BEM and analytical solutions. The sound pressure level (SPL) normalized with that at a distance of 1 m in a free field was calculated at one-fifteenth octave band center frequencies. Firstly, the comparison was carried out for a rigid semi-circular barrier of 0·125 m radius, which corresponds to the core cylinder of the Waterwheel investigated in the following section. A line source generating pure tones and a receiver were located on the ground; the line source was located at a horizontal distance of 1 m (from the axis of the barrier) in front of the barrier, and the receiver was located at a distance of 3 m behind the barrier. An analytical analysis for a rigid cylinder of 0·25 m diameter floating in the free field was carried out for comparison with results of reference [8]. Figure 4 shows that the difference between the results by BEM and the analytical solution is smaller than 0·01 dB in the frequency range below 1·6 kHz, and that BEM calculation works quite accurately. It is also shown, however, that discrepancies were observed at some frequencies above 1·6 kHz. This numerical difficulty is caused by the non-uniqueness problem; the integral equation has more than one solution at these frequencies which are close to the

eigenfrequencies of the interior boundary value problem [6]. The eigenfrequencies are decided by the shape of the boundary and appear in lower frequency range when the cross-sectional area bounded by S is large.

Secondly, the frequency characteristics of the SPL behind a rigid simple barrier of 3 m height was calculated by using the two methods. As a reference, the analytical solution derived by the diffraction theory for a half plane of zero thickness [8] was applied to four diffraction paths from a real or imaginary line source to a real or imaginary receiver. This mirror image method is often used as an exact analysis to calculate the sound field around a noise barrier built on the ground. A line source was located at a horizontal distance of 5 m in front of the barrier, and a receiver was located at a distance of 25 m behind the barrier. Both of them were set on the ground surface, hence the four diffraction paths in the exact analysis come to be the same. BEM calculations were carried out for barriers of two thicknesses; 0·0025 m which is sufficiently small to be compared with the exact analysis assuming zero thickness, and 0·03 m which is the thickness of all barriers in the following sections. Figure 5 shows the comparison of the three results. In the frequency range below 500 Hz, the middle of fluctuations of the BEM results almost correspond to the results using the analytical solution, whereas it is still unclear that the fluctuation does not appear in the analytical solution curve. Above 500 Hz, both of the BEM results are always a little smaller than the analytical result because the barrier thickness increases the sound shielding efficiency of the barrier. However, the difference between BEM results for 0·0025 m thickness and analytical results is less than 0·2 dB and small enough to conclude that the BEM calculation can yield reasonable sound field analyses around noise barriers.

Figure 5 also shows that the numerical difficulty of the discrepancies between BEM and analytical analyses does not occur in the cases of a simple and thin barrier since the small cross-section of the barrier shifts the eigenfrequencies upward. That is, one can avoid the difficulty when the thickness of the barrier is

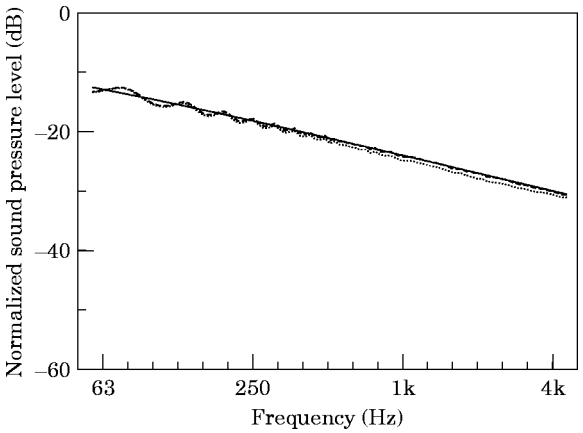

Figure 5. Comparison between BEM and an exact solution: SPL behind a hard simple barrier of 3 m height. ——, an exact solution for a half plane [8] and a mirror image method; ----, 0·0025 m thickness using BEM; . . . , 0·03 m thickness using BEM.

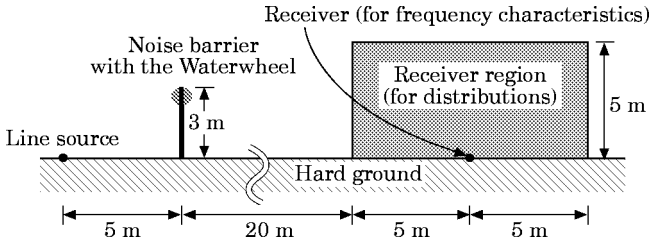

Figure 6. Geometries of a line source, noise barrier, and receivers.

sufficiently smaller than the height. The thickness of all barriers analyzed in this paper, 0·03 m, is thin enough to avoid the problem. However, when the Waterwheel cylinder is installed on the barrier, the cross-section of the barrier increases and thus the eigenfrequencies appear in the frequency range where the numerical analyses are carried out in this paper, from 63 Hz–4 kHz. If the frequency where BEM calculation is carried out happens to be very close to one of the eigenfrequencies, the result of BEM is unreliable. That is, when a calculated result at a certain frequency protrudes significantly from the frequency characteristic curve of the SPL, it might be caused by the numerical difficulty, especially in higher frequency range. Although different kinds of methods to improve this numerical difficulty around the eigenfrequencies have been proposed (most of them are based on the CHIEF method by Schenck [9] or the linear combined integral equation method by Burton and Miller [10]), the improvement of the difficulty was not adopted in this paper. This is because some of the methods are computationally expensive to implement, and others are quite simple but are not always successful.

4. IMPROVEMENT OF THE SOUND SHIELDING EFFICIENCY OF A NOISE BARRIER

The sound shielding efficiency of the noise barrier on the ground with the Waterwheel is investigated. It has been shown previously that the efficiency of a half plane with the Waterwheel is highly frequency dependent because of the strong frequency dependence of the acoustic properties of the Waterwheel surface [5]. Therefore it is expected that the efficiency of the noise barrier built on the ground is also frequency dependent, corresponding to the surface sound pressure of the Waterwheel. Figure 6 shows the cross-section of the sound field to be calculated numerically by using BEM. It is assumed that the cross-sectional shape of a noise barrier does not vary along its length. A rigid noise barrier of infinite length, 3 m height and 0·03 m thickness was positioned on the reflecting ground. The 0·03 m thickness is unrealistically small given that 0·125 m thick barriers are typically used in Japan. The 0·03 m dimension is used, however, to correspond to the thickness of the material used in scale model experiments in section 7, and consequently the numerical difficulty described previously is avoided. A coherent monofrequency line source was placed on the ground surface at a horizontal distance of 5 m in front of the barrier. SPL was calculated behind the barrier with and without the Waterwheel. The frequency characteristics of the SPL were

calculated at a receiver located on the ground surface at a distance of 25 m behind the barrier. The line source and the receiver were placed on the ground surface to avoid complications due to interference resulting from ground reflections in the monofrequency sound field. If the interference were to minimize the sound pressure at a receiver off the ground, one would not be able to distinguish the sound shielding efficiency of the barrier and the effect of the interference. The spatial distribution of the SPL was calculated in the receiver region as shown in Figure 6, with the receivers set in an array (51 $\times$ 26) at intervals of 0·2 m.

The Waterwheel cylinder was installed on the edge of a barrier. Figure 7 shows the cross-section around the edge. Both of the barriers with and without the Waterwheel were 3 m high, in order to exclude the effect of the extra barrier height from the effect of the Waterwheel. The thickness of the edge actually increases even if the height remains constant; thus, the geometrical boundary of diffraction moves upward and the so-called "effective height" increases. This increase in height, however, is sufficiently small, approximately 0·05 m. Thereby the efficiency changes only slightly with the increase in height. As shown in Figure 7, the barrier was inserted between two half cylinders of the Waterwheel. Thus, the cross-section of the edge with the Waterwheel becomes an irregular circle, which affects the sound field and the efficiency of the barrier only a little. The depth of the channels was 170 mm, corresponding to a quarter of the wavelength at 500 Hz. Taking into account the size of materials of the 1/10 scale model to be made later, the diameter of the core cylinder was 250 mm and the thickness of the plates partitioning the channels was 10 mm. Consequently, the diameter of the whole Waterwheel was 590 mm. The opening angle of the channels was 15 degrees. The channels must be sufficiently narrow when compared to the wavelength, for the sound wave needs to propagate only in the direction parallel to the radius. The 15° angle is the minimum value that allows for easy construction of the scale model. All surfaces, including the barrier with the Waterwheel and the ground, are reflective.

The frequency characteristics of the SPL behind the barriers with and without the Waterwheel were calculated using the BEM. The complicated cross-sectional

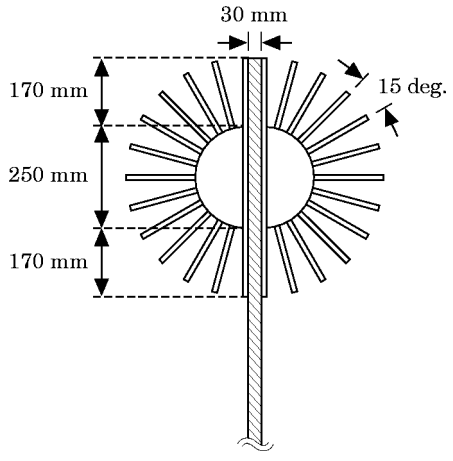

Figure 7. Cross-section of the Waterwheel installed on the barrier's edge.

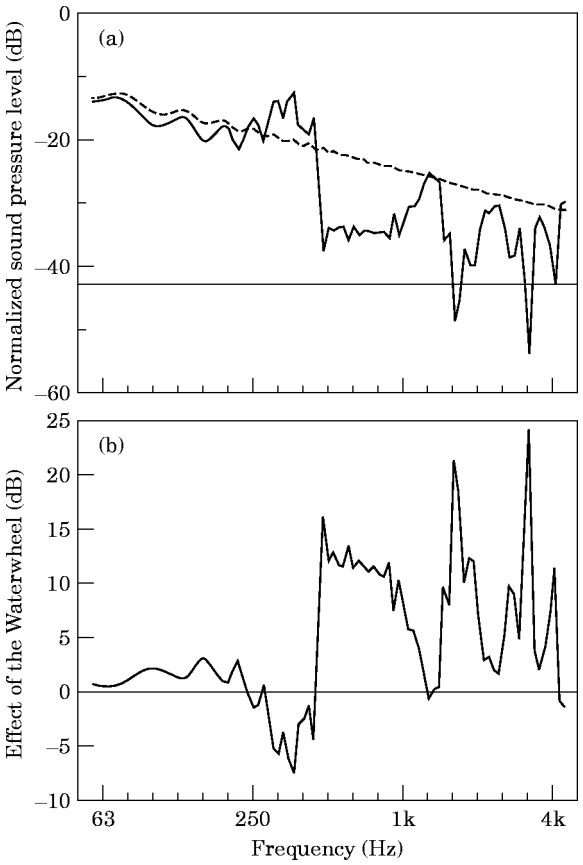

Figure 8. Frequency characteristics: (a) the sound-pressure level behind the barriers; ——, with the Waterwheel; ----, without cylinder, and (b) the effect of the Waterwheel.

shape of the barrier with the Waterwheel was divided into a large number of straight line elements, and the admittance is zero on the surface of all elements. With the Waterwheel installed on the edge, the BEM calculation might be inaccurate in the higher frequency range. This is because the core cylinder of the Waterwheel increases the thickness of the object (i.e., the barrier), and thus the non-uniqueness problem occurs in the frequency range of interest. The frequency of the pure tone generated by the line source was set at 1/15 octave intervals. Figure 8(a) shows the frequency characteristics of the SPL behind the barriers with and without the Waterwheel. One refers to the SPL difference between the barriers with and without the Waterwheel as the effect of the Waterwheel. It is shown in Figure 8(b); positive values indicate the improvement of the efficiency, that is, the decrease of the SPL by the Waterwheel. In the frequency range of 500–800 Hz, the improvement in the sound shielding exceeded 10 dB. As was described in the section 2, the surface sound pressure of the isolated Waterwheel floating in a free field is minimized (i.e., the surface becomes soft) at around the frequencies $600 + 1000n$ Hz. The efficiency improvements in the frequency ranges centred at 600 Hz and 1·6 kHz agree with the previously reported results. In a higher frequency range, however, there is no obvious relationship between the frequencies

that improve the sound shielding efficiency and those that make the surface soft, especially at 3·2 kHz. This is partly because the BEM yields inaccurate predictions due to the non-uniqueness problem. As shown in section 3, the non-uniqueness problem is caused in the frequency range above 2·7 kHz in the case of the rigid semi-circular barrier of 0·125 m radius. In consequence, the problem could be caused when the sound field around the barrier with the Waterwheel including a rigid core cylinder of 0·125 m radius is calculated. On the other hand, the effect of the Waterwheel is negative in the range of 315–400 Hz. This negative effect is remarkably large, more than 5 dB at maximum, and corresponds to an increase in the surface sound pressure of the Waterwheel. In a manner similar to that discussed for a half-plane with the Waterwheel in the previous report, the Waterwheel increases the sound energy diffracted into the back of the barrier.

Spatial distribution of the SPL and the Waterwheel's effect was calculated in the back of the barrier. The calculation was carried out in the region of 20 m to 30 m horizontally from the barrier and ground surface to 5 m high, as shown in Figure 6. The frequency was set at 630 Hz to make the Waterwheel's surface soft.

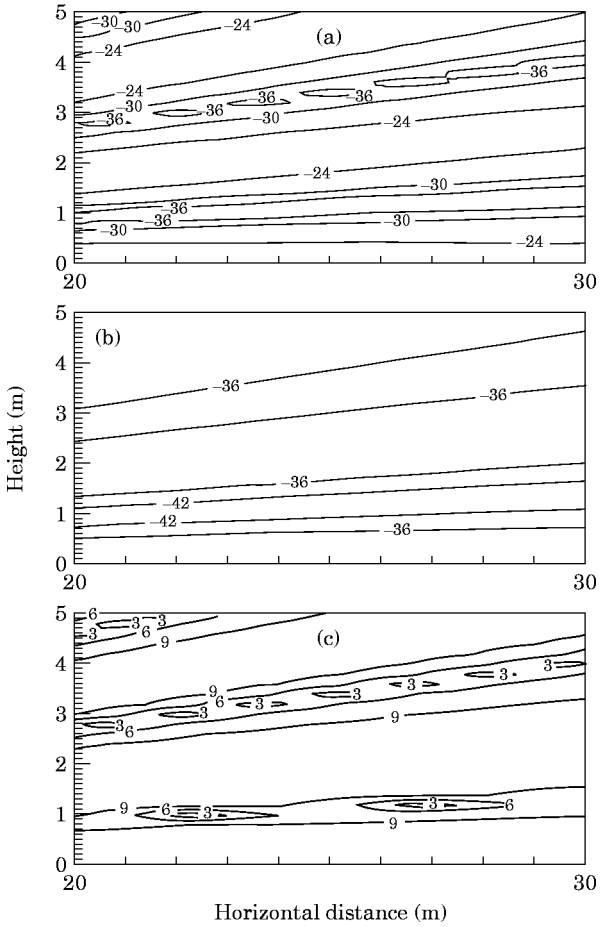

Figure 9. Spatial distributions behind the barrier at 630 Hz: (a) sound pressure level without cylinder, (b) sound pressure level with the Waterwheel, and (c) effect of the Waterwheel.

Figures 9(a) and (b) show the SPL distribution behind the barrier without (a) or with (b) the Waterwheel. Values in both figures indicate SPL normalized with that at a distance of 1 m in a free field, and contour lines are drawn at 6 dB intervals. As shown in Figure 9(a), there are three SPL dips where the difference between two path lengths from real and imaginary barrier edges to the receiver correspond to a half of the wavelength multiplied by odd numbers. In other words, the SPL dips are caused by reflections from the hard ground. Figure 9(c) shows the effect of the Waterwheel, which is the difference between the two SPLs. Positive values in Figure 9(c) indicate improvement of the sound shielding efficiency, and the contour lines are drawn at 3 dB intervals. It is shown that the large decrease in the SPL, more than 9 dB, covers a broad region. The region where the efficiency improvement is small corresponds to the region in which the SPL dips, due to interference caused by the ground reflection, as shown in Figure 9(a). That is, the Waterwheel does not improve the sound shielding efficiency, in the region where the SPL was small even if the Waterwheel was not installed.

The energetic average (rather than the arithmetic average) of the SPL behind the barrier is discussed below. Let the energetic average of the SPL, $\bar{L}$, be defined as $\bar{L} = 10 \log_{10} \{(10^{L_1/10} + \cdots + 10^{L_N/10})/N\}$ where L_i denotes the SPL at the ith receiver and N denotes the total number of the receivers. Calculated $\bar{L}$ is $-25{\cdot}0$ dB behind the barrier without the Waterwheel, decreasing to $-34{\cdot}5$ dB when the Waterwheel is installed. Consequently, the averaged effect of the Waterwheel in the region of interest (i.e., the difference of the two SPL averages) is 9·5 dB.

5. CROSS-SECTIONAL SHAPE OF THE WATERWHEEL

This section discusses the relationship between the cross-sectional shape of the Waterwheel and the improvement in the sound shielding efficiency. The change of the efficiency that results from the change of the depth of the channels, the opening angle of the channels, and the whole diameter of the Waterwheel is calculated using the BEM. The calculations were carried out using pure tones at 1/15 octave frequency intervals.

5.1. DEPTH OF THE CHANNEL

The depth of the channels of the Waterwheel discussed in the previous section was 170 mm, equal to a quarter of the wavelength at 500 Hz. As mentioned previously, the sound shielding efficiency of the barrier improves most in the frequency range centered at approximately 600 Hz. The depth was changed to 100 mm (one-quarter of the wavelength at 850 Hz), with the diameter of the whole Waterwheel kept at 590 mm; consequently, the diameter of the core cylinder was 390 mm. Figure 10 shows the calculated effect of the Waterwheel. As expected, the frequency range of the improvement shifted to a higher range and was centred at approximately 1 kHz. Although the positive effect of the 100 mm channel was the same as that of the 170 mm channel, the width of the ineffective range was wider. As is shown in the next section, the width of the negative effect range is related to the ratio of the depth to the diameter of the Waterwheel.

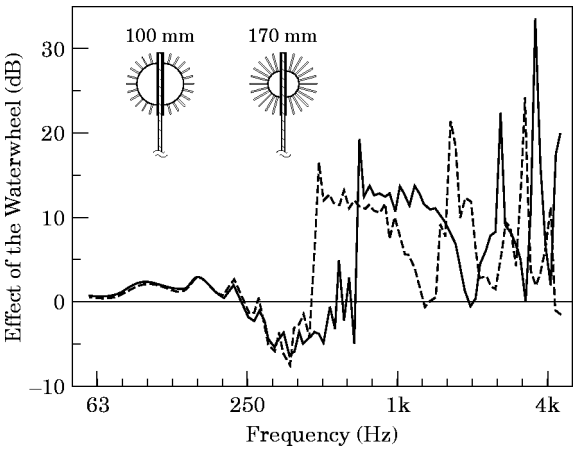

Figure 10. Difference of the Waterwheel's effect caused by the variations of channel depth. ——, 110 mm; ----, 170 mm.

5.2. DIAMETER OF THE WATERWHEEL

The sound shielding efficiency of the barrier with Waterwheels of different diameters is discussed. The diameter of the whole Waterwheel varied from the original size of 590 mm to 490 mm, 690 mm, and 790 mm, with the depth of the channels kept at 170 mm. The ratio of the area of the open end of the channel to that of the bottom is 5·6:1 for the 490 mm Waterwheel and 1·9:1 for the 790 mm one; hence the channels of the 790 mm Waterwheel are fairly rectangular in shape as compared to that of the 490 mm.

Results of the calculations are shown in Figure 11. The frequency width of the improvement around 630 Hz is discussed below. It was expected that the whole of the improved frequency band would shift to a lower frequency. Nonetheless, only the lower limit of the band shifted to a lower frequency while the higher limit

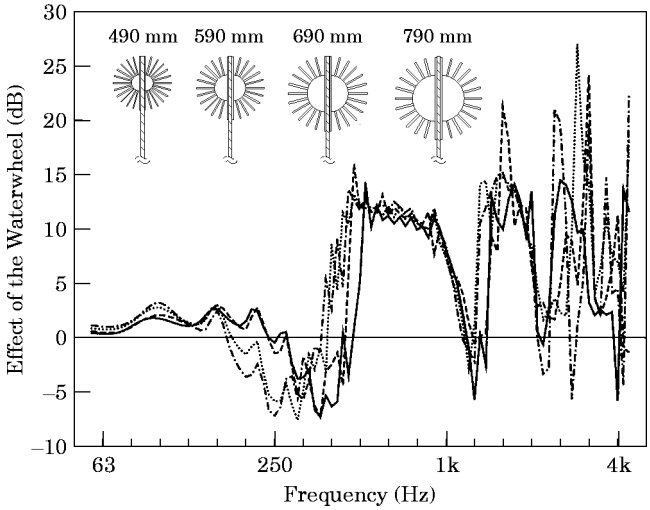

Figure 11. Difference of the Waterwheel's effect caused by the variations of its diameter. ——, 490 mm; ----, 590 mm; . . . . , 690 mm; —·—·—, 790 mm.

remained the same. On the other hand, the range of the negative effect shifted down as a whole. Furthermore, the band width of the negative effect became broader with increasing diameter. As mentioned in the previous section, the ratio of the depth to the diameter of the Waterwheel affects the width of the negative effect range.

It was also expected that the maximum value of the effect would increase with an increasing diameter, because of an increase of the soft surface. The results indicate, however, that the maximum value of the effect changed only slightly, whereas the width of the effective range increased substantially. The soft surface area increased when the diameter of the Waterwheel increased; nevertheless, the soft surface extended away from the edge. In other words, the soft surface area does not increase in the region close to the edge, and therefore the increasing diameter does not affect the amplitude of the edge potential and the sound field behind the barrier. The diameter affects only the shape of the Waterwheel channels that determine the width of the effective range.

Results above 2 kHz are quite chaotic and it is difficult to find any trend. As mentioned in the section 4, the non-uniqueness problem is caused above 2·7 kHz. Furthermore, the problem might happen in a lower frequency range when the core cylinder of the Waterwheel is larger than the original.

5.3. OPENING ANGLE OF THE CHANNEL

In this study, the opening angle of the channel was 15°; that is, a circle was divided into 24 sectors. The 15° angle was set to propagate the sound waves in the channels parallel to the radius of the Waterwheel. Generally speaking, in the duct of a constant cross-sectional area, the sound wave propagates as a plane wave when the inner diameter of the duct is smaller than half of the wavelength. For the required propagation in the channel of the Waterwheel, however, the upper limit of the cross-section area was not obtained. The 15° angle was the minimum value that allowed for easy construction of the two-dimensional scale model [5], and there were no physical foundations to decide the angle.

With the depth of channels kept at 170 mm and the diameter kept at 590 mm, the effect of the Waterwheel was calculated for different opening angles. The opening angle was set at 15, 20, 30, 36, and 45°, which is 180° divided by the integers 12, 9, 6, 5, and 4. Figure 12 shows the effect of change in the opening angle on the effect of the Waterwheel. In the frequency range under 400 Hz, the negative effect changed only slightly. In contrast, the form of the graphs above 1 kHz differs significantly for each opening angle, and thus no noticeable relationship between the opening angle and the efficiency improvement was found. In the higher frequency range, the sound wave in a channel does not propagate solely parallel to the radius of the Waterwheel, i.e., the Waterwheel surface is not locally reactive, because the channel mouth is no longer smaller than half of the wavelength. For example, in the case of the 30° opening angle, the mouth of each channel exceeds half of the wavelength at around 1·2 kHz. Accordingly, one cannot easily estimate the acoustical property of the Waterwheel surface in this frequency range.

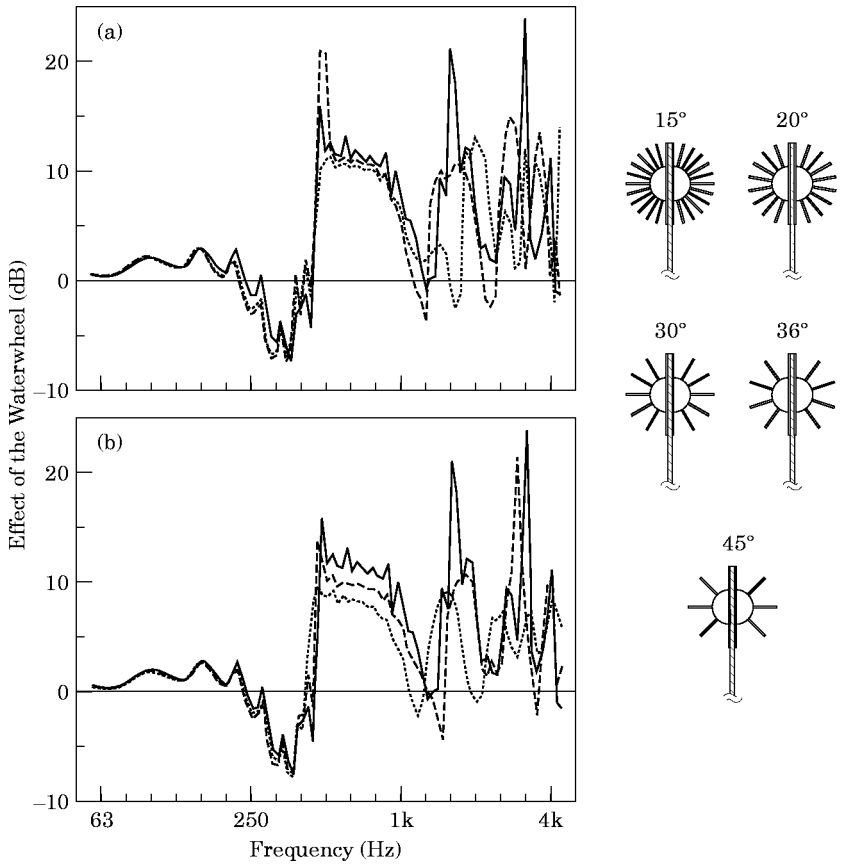

Figure 12. Difference of the Waterwheel's effect caused by the variation of the channel opening angle: (a) ——, 15°; ----, 20°; . . . . , 30°; (b) ——, 15°; ----, 36°; . . . . , 45°.

The effect of the Waterwheel in the range of 500 Hz–1 kHz is discussed below. The effect decreases with an increasing opening angle. When the opening angle is less than 36°, the decrease of the effect is less than 2 dB. The effect decreases by 4 dB, however, with the opening angle set at 45°. Even if the opening angle increases from 15–36°, that is, even if the number of the plates decreases to half of the original, the effect decreases by only 2 dB. Nevertheless, when only two more plates are omitted (i.e., a 45° opening), the effect decreases by 4 dB as compared to that of the 15° opening. For practical use of the noise barrier with the Waterwheel, a compromise between the weight of the Waterwheel and the sound shielding efficiency must be found. Consequently, the channels of the Waterwheel considered in this study should be narrower than 36°. The limit of the opening angle is also related to other dimensions, e.g., the diameter of the Waterwheel and the depth of the channels. As such, further investigation is needed.

6. COMPARISON WITH DIFFERENT CYLINDERS

The effect of the Waterwheel cylinder is compared to that of a hard cylinder, an absorbing cylinder, and a soft cylinder. In this section, one refers to the term

"absorbing" as the surface of ρc impedance, and the term "soft" as the surface of zero impedance, both regardless of the frequency. Consider a cylinder of 590 mm in diameter installed on the edge of a 3 m high rigid barrier. The dimensions of the Waterwheel used for the comparison are: diameter, 590 mm; depth of the channels, 170 mm; and opening angle, 15°. The source and receiver geometry was the same as shown in Figure 6.

Figure 13 shows the difference of the SPL behind the noise barrier with and without each of the cylinders, i.e., the improvement in the noise shielding efficiency due to each cylinder. Results in the higher frequency range, especially for a soft cylinder, are doubtful because of the non-uniqueness problem of the BEM. A hard cylinder improves the efficiency by up to 3 dB in the lower frequency range; however, the effect in the middle and higher ranges was nearly zero. When the surface of the cylinder becomes absorbing and soft, a larger improvement in efficiency is gained. Even though the acoustic properties of the absorbing and soft surfaces were not frequency dependent, the effect of these cylinders increased with increasing frequency. This is because the region where the edge potential decreases becomes larger as compared to wavelengths with increasing frequency. At 630 Hz, the Waterwheel produces nearly the same improvement as a soft cylinder. Except for the negative effect in the range of 315–400 Hz, the value of the SPL ranges from those of a hard cylinder to those of a soft cylinder. Consequently, the hypothesis that the acoustic properties of the surface of the Waterwheel converge between that of hard and soft surfaces because of the nature of the interference is supported. This hypothesis, however, cannot illustrate the behavior of the Waterwheel in the range of 315–400 Hz. A method to avoid the negative effect might be found if the unexpected sound field around the Waterwheel in the frequency range can be analyzed.

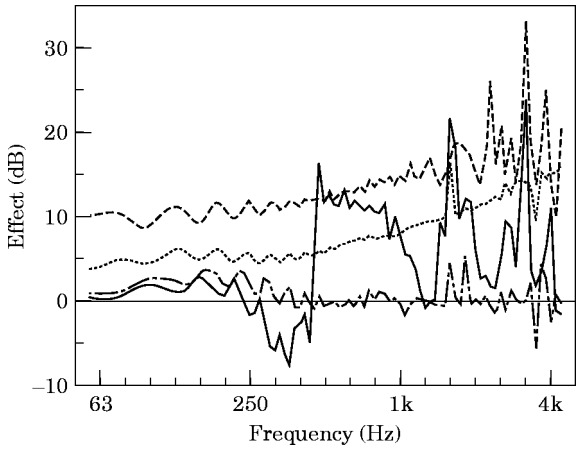

Figure 13. Improvement in the barrier's efficiency by different cylinders. ——, with the Waterwheel; ----, with a soft cylinder; . . . . , with an absorbing cylinder; –·–·–, with a hard cylinder.

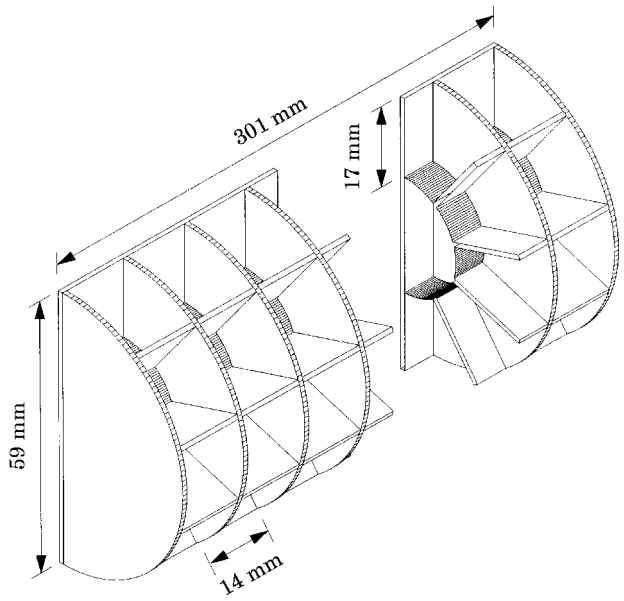

Figure 14. Scale model of the Waterwheel for three-dimensional experiments.

7. EXPERIMENTAL RESULTS

All of the above findings were determined from numerical analyses using two-dimensional BEM. It has been already reported that the numerical analyses assuming the two-dimensional sound field can provide a good indication of the three-dimensional experiment using a point source when the point source and the receiver in the experiment are in the vertical plane which is perpendicular to the axis of the noise barrier [6]. In this section, three-dimensional experiments are performed to confirm that the two-dimensional simulations accurately predict three-dimensional sound fields.

A scale model of the Waterwheel was constructed as shown in Figure 14. The dimensions in the experiments were reduced to a scale of one-tenth, and thus the depth of the wells was 17 mm and the diameter of the core cylinder was 25 mm. The core cylinder was made of a half pipe of 1·5 mm thick aluminum, and the rest of the parts were 1 mm thick aluminum plates. Transmission loss (TL) of these materials was large enough not to harm the sound field. The opening angle of the wells was 36° by taking into account the results shown in Figure 12. The opening width along the longitudinal direction of the cylinder was 14 mm, which is half of the wavelength at 12 kHz, to make the Waterwheel surface (i.e., the open ends of the wells) approximately locally reactive under the frequency. One unit was 301 mm long with a diameter of 59 mm. Twenty-four models were constructed, thus obtaining a Waterwheel cylinder with a total length of 3·6 m.

Scale model experiments were carried out in a hemianechoic room. The geometry of the barrier, point source, and receivers is shown in Figure 15. A 300 mm high noise barrier was sitting on the rigid floor, and the Waterwheel was installed on the edge. The barrier was inserted between two half cylinders of the Waterwheel, similar to Figure 7. Though the line source was on the ground surface

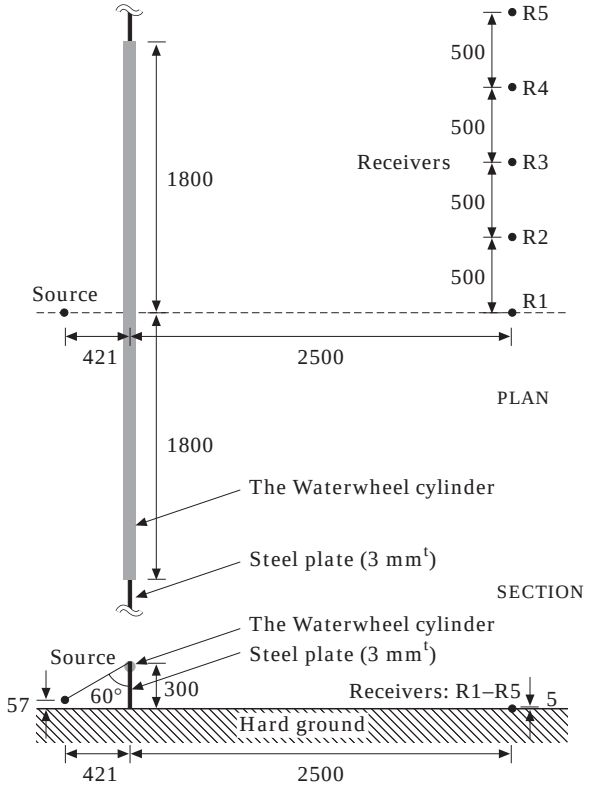

Figure 15. Configurations of experiments in a hemianechoic room.

in the previous simulations, the point source in the present experiment was above the ground because of the size of the loudspeaker. A corn speaker was used for the frequency range of 630 Hz–2·0 kHz, and a tweeter for the range above 2·5 kHz. A 1/4 in condenser microphone was set at a height of 5 mm, and the microphone head faced the floor downward and vertically to exlclude its directivity. Pink noise was generated to measure the 1/3 octave band SPL. As in the sections above, one refers to the difference of the SPL behind the barrier with and without the Waterwheel as the effect of the cylinder.

Figure 16 shows the results of the experiments, and illustrates that the sound shielding efficiency of the noise barrier improves by approximately 10 dB in the range of 5–8 kHz despite the negative effect at 3·15 kHz and 4 kHz. In the range of 16–40 kHz, the improvement occurs at receivers R1 to R3. However, the effect is fairly small at R4 and R5. The largest improvement due to the Waterwheel in the higher frequency range was gained when a source and a receiver are set along the line perpendicular to the barrier, and the improvement decreased when the source and receiver were moved away from the perpendicular.

To achieve a meaningful comparison, the effect of the Waterwheel was calculated again using two dimensional BEM for the cross-sectional geometry shown in Figure 15. First the SPLs were calculated using pure tones at frequency intervals of 1/15 octave, and the five results around the center frequency of a 1/3 octave band were averaged energetically to approximate the 1/3 octave band SPL.

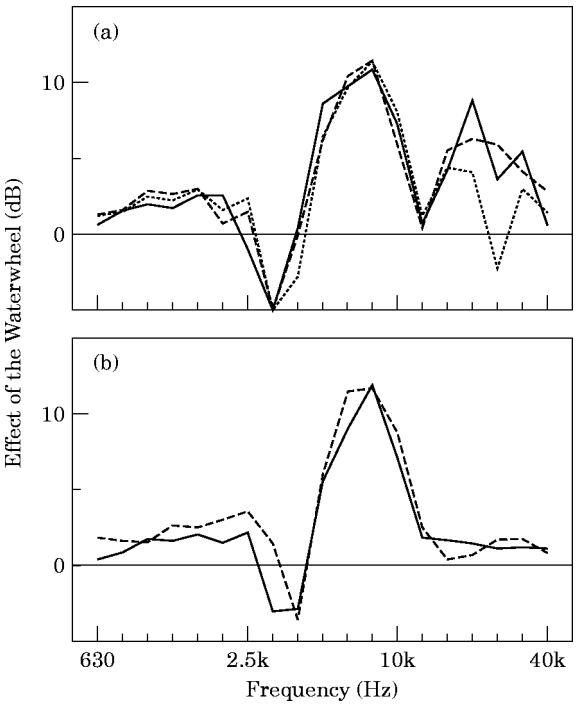

Figure 16. Measured effect of the Waterwheel cylinder during 1/10 scale model experiments: (a) ——, at receiver R1; ----, at receiver R2; . . . . , at receiver R3, and (b) ——, at receiver R4; ----, at receiver R5.

The difference between the approximated band SPLs behind the barrier with and without the Waterwheel is the effect of the cylinder. The comparison is shown in Figure 17, with frequencies in the abscissa converted to the real scale. The results of the experiment and simulation agree, despite the difference in the two-dimensional and three-dimensional method, except in the range above

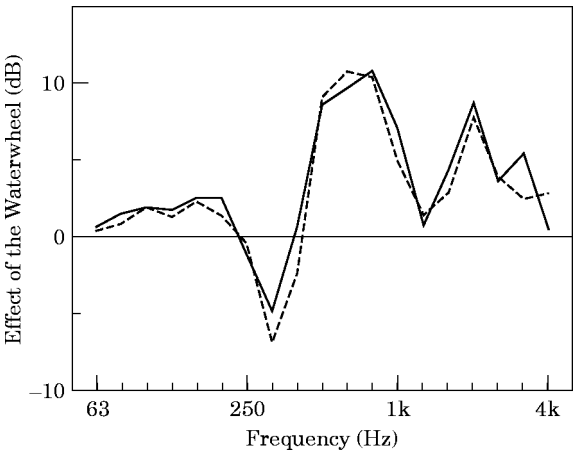

Figure 17. Comparison between three-dimensional experiment at the receiver R1 (——) and two-dimensional BEM simulation (----): effect of the Waterwheel.

3·15 kHz where the non-uniqueness problem of BEM might decrease the accuracy. It is concluded that the two-dimensional numerical analyses can estimate the sound shielding efficiency of noise barriers with the Waterwheel in a three-dimensional sound field. The two-dimensional numerical analyses, however, cannot estimate the angle dependence of the effect of the Waterwheel, as demonstrated in the results for R4 and R5. Therefore, three-dimensional experiments are still needed to predict the angle dependence.

8. CONCLUSIONS

The sound shielding efficiency of a noise barrier sitting on the ground and the improvement of the efficiency by the Waterwheel installed on the edge of the barrier were investigated. The frequency characteristics of the sound shielding efficiency indicate that the efficiency increases by more than 10 dB in the frequency range where the surface sound pressure of the Waterwheel is minimized, and the width of the effective range is approximately one octave. On the other hand, in the range where the sound pressure of the surface of the Waterwheel is larger than that of a rigid cylinder, the Waterwheel produces a negative effect. Spatial distribution of the effect was calculated at the frequency that produces minimal sound pressure at the surface of the Waterwheel. Consequently, it was shown that the effect was nearly 10 dB on average in the region investigated.

The relationship between the cross-section of the Waterwheel and its effect was discussed. The depth of the channels and the diameter of the whole Waterwheel influence the center frequency and the lower limit of the frequency range where the efficiency improvement occurs. Furthermore, the opening angle of the channel affects the upper limit of the effective range. The above investigations were based on two-dimensional numerical analyses, and therefore three-dimensional experiments were performed to confirm the accuracy of the simulations. Results of the scale model experiment in an hemianechoic chamber show that the Waterwheel is effective in the three-dimensional sound field, and that the two-dimensional simulations can approximate the effect of the Waterwheel in the three-dimensional field. In addition, the effect of the Waterwheel in a higher frequency range is dependent on the incident angle.

The extension of the effective range and the reduction of the negative effect are currently being investigated in the application of the Waterwheel to practical noise control. A Waterwheel with different channel depths is expected to improve the efficiency of the noise barrier. Moreover, intensity analysis might be very helpful in determining the reason why the Waterwheel improves the sound shielding efficiency of the barrier while completely reflecting the sound energy.

REFERENCES

1. K. FUJIWARA and N. FURUTA 1991 *Noise Control Engineering Journal* **37**, 5–11. Sound shielding efficiency of a barrier with a cylinder at the edge.
2. K. FUJIWARA 1990 *Proceedings of Internoise* '90, 343–346. Sound shielding efficiency of a barrier with soft surface.

3. J. B. KELLER and D. G. MAGIROS 1961 *Communication in Pure and Applied Mathematics* **14**, 457–471. Diffraction by a semi-infinite screen with a round end.
4. A. D. RAWLINS 1976 *Journal of Sound and Vibration* **45**, 53–67. Diffraction of sound by a rigid screen with a soft or perfectly absorbing edge.
5. T. OKUBO and K. FUJIWARA *Journal of Acoustical Society of Japan* (*E*) **19**, 187–197. Efficiency of a noise barrier with an acoustically soft cylindrical edge.
6. D. C. HOTHERSALL, S. N. CHANDLER-WILDE and M. N. HAJMIRZAE 1991 *Journal of Sound and Vibration* **146**, 303–322. Efficiency of single noise barriers.
7. R. SEZNEC 1980 *Journal of Sound and Vibration* **73**, 195–209. Diffraction of sound around barriers: use of the boundary elements technique.
8. J. J. BOWMAN, T. B. A. SENIOR and P. L. E. USLENGHI 1969 *Electromagnetic and Acoustic Scattering by Simple Shapes*. Amsterdam: North-Holland.
9. H. A. SCHENCK 1968 *Journal of Acoustical Society of America* **44**, 41–58. Improved integral formulation for acoustic radiation problems.
10. A. J. BURTON and G. F. MILLER 1971 *Proceedings of the Royal Society of London* **A323**, 201–210. The application of integral equation methods to the numerical solutions of some exterior boundary value problems.